

Sphaleron And Critical bubble in a scale invariant model : ReAnalysis

Kaori Fuyuto^{1*} and Eibun Senaha^{1,2†}

¹*Department of Physics, Nagoya University, Nagoya 464-8602, Japan and*

²*Department of Physics and Center for Mathematics and Theoretical Physics,
National Central University, Taoyuan, 32001, Taiwan*

(Dated: January 28, 2022)

We revisit the electroweak phase transition and the critical bubble in the scale invariant two Higgs doublet model in the light of recent LHC data. Moreover, the sphaleron decoupling condition is newly evaluated in this model. The analysis is done by using the resummed finite-temperature one-loop effective potential. It is found that the 125 GeV Higgs boson inevitably leads to the strong first-order electroweak phase transition, and the strength of which is always large enough to satisfy the sphaleron decoupling condition, $v_N/T_N > 1.2$, where T_N denotes a nucleation temperature and v_N is the Higgs vacuum expectation value at T_N . In this model, even if the Higgs boson couplings to gauge bosons and fermions are similar to the standard model values, the signal strength of the Higgs decay to two photons is reduced by 10% and the triple Higgs boson coupling is enhanced by 82% compared to the standard model prediction.

I. INTRODUCTION

One of the observational facts that needs new physics beyond the standard model (SM) is the baryon asymmetry of the Universe (BAU) [1],

$$\frac{n_B}{s} = (8.59 \pm 0.11) \times 10^{-11} \quad (\text{Planck}) \quad (1)$$

where n_B (s) denotes the baryon number (entropy) density. Although many mechanisms that can explain the observed value exist in the literature, electroweak baryogenesis (EWBG) [2] is the only scenario that is ripe for verification by collider experiments, such as the Large Hadron Collider (LHC), and by low energy experiments, such as the electric dipole moments of the neutron, atoms and molecules. Since EWBG is intimately connected to Higgs physics, the establishment of the Higgs sector plays an essential role in testing it, and the discovery of the Higgs boson at the LHC in 2012 [3, 4] is the first step toward the collider probe of EWBG. Indeed, since the Higgs boson mass that is one of the relevant parameters for the electroweak phase transition (EWPT) has been measured with 0.2% accuracy, $m_H = 125.09 \pm 0.21$ (stat.) ± 0.11 (syst.) GeV [5], the feasible regions of EWBG have been narrowed down in various models [6]. In upcoming experiments, such as the LHC Run-II and the High-Luminosity LHC [7], the Higgs boson couplings to the SM particles would be measured with better precision, and the international linear collider (ILC) [8] has the great capability of measuring the triple Higgs boson coupling, which may yield a decisive clue to the EWBG hypothesis.

In order for EWBG to be successful, the EWPT has to be strongly first order. The properties of the EWPT are related not only to the Higgs boson mass and model

parameters but also to electroweak symmetry breaking mechanisms. An interesting possibility is the so-called Coleman-Weinberg (CW) mechanism [9, 10] in which quantum effects induce the symmetry breaking. The scale invariant two Higgs doublet model (SI-2HDM) [11–16] is one of such examples,¹ and the previous work [12] shows that the SI-2HDM can have the strong first-order EWPT. At the time of their analysis, however, the masses of the Higgs boson and top quark were not known. Moreover, on the theoretical front, neither a thermal resummation for the effective potential nor the evaluation of a baryon number preservation condition (also called a sphaleron decoupling condition) were conducted in Ref. [12].

In this Letter, we update the analysis of the EWPT including the evaluation of bubble wall profiles, and obtain the sphaleron decoupling condition by taking the recent LHC data into account. In our study, we use the finite-temperature one-loop effective potential with daisy resummation. The phenomenological consequences of the sphaleron decoupling condition is also briefly discussed. As studied in the previous works [17, 18], we evaluate the deviations of the Higgs boson couplings from their SM values in the region where the strong first-order EWPT is achieved.

The paper is organized as follows. We give a quick review of the SI-2HDM in section II, and the Higgs boson couplings are presented in section III. The sphaleron decoupling condition and the critical bubbles are discussed in section IV. We show our results in section V, and conclusions and discussions are given in section VI.

* fuyuto@th.phys.nagoya-u.ac.jp

† senaha@ncu.edu.tw

¹ The CW mechanism does not work in the SM since the top quark is too massive to give the stable vacuum.

II. THE MODEL

The SI-2HDM is a minimal scale invariant extension of the SM by adding another Higgs doublet field. The most general Higgs potential at the renormalizable level is given by

$$V_0 = \frac{\lambda_1}{2}(\Phi_1^\dagger \Phi_1)^2 + \frac{\lambda_2}{2}(\Phi_2^\dagger \Phi_2)^2 + \lambda_3(\Phi_1^\dagger \Phi_1)(\Phi_2^\dagger \Phi_2) + \lambda_4(\Phi_1^\dagger \Phi_2)(\Phi_2^\dagger \Phi_1) + \left\{ \frac{\lambda_5}{2}(\Phi_1^\dagger \Phi_2)^2 + \lambda_6(\Phi_1^\dagger \Phi_1)(\Phi_1^\dagger \Phi_2) + \lambda_7(\Phi_2^\dagger \Phi_2)(\Phi_1^\dagger \Phi_2) + \text{h.c.} \right\}. \quad (2)$$

After two Higgs doublets get vacuum expectation values (VEVs), they are cast into the form

$$\Phi_i(x) = \left(\frac{\phi_i^+(x)}{\sqrt{2}}(v_i + h_i(x) + ia_i(x)) \right), \quad i = 1, 2, \quad (3)$$

where $v_1 = v \cos \beta$ and $v_2 = v \sin \beta$ with $0 \leq \beta \leq \pi/2$, and $v \simeq 246$ GeV. In order to avoid Higgs-mediated flavor changing neutral current (FCNC) processes at the tree level, we impose a Z_2 symmetry ($\Phi_1 \rightarrow -\Phi_1$, $\Phi_2 \rightarrow \Phi_2$), which leads to $\lambda_6 = \lambda_7 = 0$ [19]. The phase of λ_5 is removed by an appropriate field redefinition of the Higgs doublets, so that CP is conserved.

Following a method by Gildener and Weinberg [10], we consider the EW symmetry breaking in a flat direction. The tree-level effective potential takes the form

$$V_0(\varphi_1, \varphi_2) = \frac{\lambda_1}{8}\varphi_1^4 + \frac{\lambda_2}{8}\varphi_2^4 + \frac{\lambda_{345}}{4}\varphi_1^2\varphi_2^2, \quad (4)$$

where φ_1 and φ_2 are the constant background fields of the two Higgs doublets.

The tadpole conditions that are defined as the first derivatives of V_0 with respect to $\varphi_{1,2}$ give the following conditions:

$$\lambda_{345} + \sqrt{\lambda_1 \lambda_2} = 0, \quad \lambda_1 v_1^4 = \lambda_2 v_2^4, \quad (5)$$

where $\lambda_{345} = \lambda_3 + \lambda_4 + \lambda_5$. With these conditions, it follows that $V_0(v_1, v_2) = 0$. Moreover, since the mass matrix of h_1 and h_2 is written as

$$\mathcal{M}_{\text{tree}}^2 = \begin{pmatrix} \lambda_1 v_1^2 & \lambda_{345} v_1 v_2 \\ \lambda_{345} v_1 v_2 & \lambda_2 v_2^2 \end{pmatrix}, \quad (6)$$

one finds $\det(\mathcal{M}_{\text{tree}}^2) = 0$ using Eq. (5). The appearance of the massless particle is the consequence of the classical scale invariance. We define h and H as the mass eigenstates of the CP-even Higgs bosons, which are obtained by

$$\begin{pmatrix} h_1 \\ h_2 \end{pmatrix} = \begin{pmatrix} \cos \alpha & -\sin \alpha \\ \sin \alpha & \cos \alpha \end{pmatrix} \begin{pmatrix} H \\ h \end{pmatrix}, \quad (7)$$

where $-\pi/2 \leq \alpha \leq 0$. In the following discussion, h is the SM-like Higgs boson whose mass is zero at the tree level and is generated by the quantum corrections. It can be proved that $\alpha = \beta - \pi/2$ at the tree level, and consequently, the Higgs boson couplings to the gauge bosons and fermions are the same as those in the SM.

As mentioned above, h becomes massive as the result of the radiative EW symmetry breaking. The one-loop effective potential is [9, 20]

$$V_1(\varphi) = \sum_i n_i \frac{\bar{m}_i^4(\varphi)}{64\pi^2} \left(\log \frac{\bar{m}_i^2(\varphi)}{\bar{\mu}^2} - c_i \right), \quad (8)$$

where $\varphi = \sqrt{\varphi_1^2 + \varphi_2^2}$ and $i = H, A, H^\pm, W^\pm, Z, t, b$, and $c_i = 3/2$ ($5/6$) for scalars and fermions (gauge bosons) and $\bar{\mu}$ denotes a renormalization scale. A and H^\pm are the physical CP-odd and charged Higgs bosons, respectively. n_i are the degrees of freedom and the statistics of the particle i :

$$n_H = n_A = 1, \quad n_{H^\pm} = 2, \quad n_{W^\pm} = 3 \cdot 2, \\ n_Z = 3, \quad n_t = n_b = -12. \quad (9)$$

The field-dependent masses can be written as $\bar{m}_i^2 = m_i^2 \varphi^2 / v^2$, where m_i are the corresponding masses in the vacuum, so that $V_1(\varphi)$ is reduced to

$$V_1(\varphi) = A\varphi^4 + B\varphi^4 \log \frac{\varphi^2}{\bar{\mu}^2}, \quad (10)$$

with

$$A = \sum_i n_i \frac{m_i^4}{64\pi^2 v^4} \left(\log \frac{m_i^2}{v^2} - c_i \right), \quad B = \sum_i n_i \frac{m_i^4}{64\pi^2 v^4}. \quad (11)$$

As can be seen from the tadpole condition of $V_1(\varphi)$, we have a relationship between the scale of v and the renormalization scale $\bar{\mu}$, i.e., $v^2 = \bar{\mu}^2 e^{-1/2-A/B}$, as the consequence of dimensional transmutation. From Eqs. (10) and (11), it is easily checked that the vacuum energy becomes $V_1(v) = -Bv^4/2$, which implies that the electroweak symmetry is broken unless B is negative. It should be noted that since A and B are the same order in the coupling, i.e., $\mathcal{O}(g^4)$, where g collectively denotes the coupling constants in this model, A/B should be $\mathcal{O}(1)$, so the $\log(v^2/\bar{\mu}^2) \sim \mathcal{O}(1)$. In other directions, however, A may be $\mathcal{O}(g^2)$ and thus $\log(v^2/\bar{\mu}^2) \sim 1/g^2$, which may invalidate the perturbative calculation, as advocated in Ref. [10].

The mass of h is obtained by taking the second derivative of $V_1(\varphi)$ and evaluating it at $\varphi = v$,

$$m_h^2 = \left. \frac{\partial^2 V_1(\varphi)}{\partial \varphi^2} \right|_{\varphi=v} = 8Bv^2. \quad (12)$$

We remark that thanks to the loop contributions from H, A and H^\pm , B can be positive in contrast to the SM

case, rendering m_h^2 positive. Interestingly, once $m_h = 125$ GeV is fixed, the possible ranges of m_H , m_A and m_{H^\pm} are restricted. In this Letter, we consider a case that $m_A = m_{H^\pm}$ in order to satisfy the constraint coming from the ρ parameter [21]. Therefore, the heavy Higgs mass scales are specified by only two parameters. In what follows, m_H and m_A are chosen.

III. HIGGS BOSON COUPLINGS

The Higgs boson couplings to gauge bosons and fermions normalized to the SM values are, respectively, given by

$$\kappa_V = \frac{g_{hVV}^{\text{SI-2HDM}}}{g_{hVV}^{\text{SM}}}, \quad \kappa_f = \frac{g_{hff}^{\text{SI-2HDM}}}{g_{hff}^{\text{SM}}}, \quad (13)$$

where $f = u, d, l$. As discussed in section II, $\kappa_V = \kappa_f = 1$ due to $\alpha = \beta - \pi/2$ at the tree level. Even in such a situation, the so-called nondecoupling effects may appear in the loop processes. For instance, as pointed out in Ref. [22], the $h \rightarrow \gamma\gamma$ mode may be significantly modified by the charged Higgs boson loop. The Higgs signal strength of $h \rightarrow \gamma\gamma$ is defined as

$$\mu_{\gamma\gamma} = \frac{\sigma(pp \rightarrow h)_{\text{SI-2HDM}} \text{Br}(h \rightarrow \gamma\gamma)_{\text{SI-2HDM}}}{\sigma(pp \rightarrow h)_{\text{SM}} \text{Br}(h \rightarrow \gamma\gamma)_{\text{SM}}} \simeq \left| 1 + \frac{\mathcal{A}_{H^\pm}}{\mathcal{A}_{\text{SM}}} \right|^2, \quad (14)$$

where $\mathcal{A}_{\text{SM}} = -6.49$ [23] and $\mathcal{A}_{H^\pm} = -\tau_{H^\pm}(1 - \tau_{H^\pm} f(\tau_{H^\pm}))$ with $\tau_{H^\pm} = 4m_{H^\pm}^2/m_h^2$, and f is a loop function defined in Ref. [24].

The another nondecoupling effect may appear in the triple Higgs boson coupling. The deviation of the triple Higgs boson coupling from its SM value is defined as

$$\Delta\lambda_{hhh} = \frac{\lambda_{hhh}^{\text{SI-2HDM}} - \lambda_{hhh}^{\text{SM}}}{\lambda_{hhh}^{\text{SM}}}. \quad (15)$$

In this analysis, we use the following expression as the SM prediction [25]

$$\lambda_{hhh}^{\text{SM}} = \frac{3m_h^2}{v} \left[1 + \frac{9m_h^2}{32\pi^2 v^2} + \sum_{i=W,Z,t,b} n_i \frac{m_i^4}{12\pi^2 m_h^2 v^2} \right]. \quad (16)$$

Note that the dominant one-loop contribution comes from the top quark loop, which renders λ_{hhh} smaller compared to the leading result. In the SI-2HDM, the triple Higgs boson coupling to leading order is simply expressed in terms of m_h and v [26]

$$\lambda_{hhh}^{\text{SI-2HDM}} = \frac{\partial^3 V_1(\varphi)}{\partial \varphi^3} \Big|_{\varphi=v} = 40Bv = \frac{5m_h^2}{v}. \quad (17)$$

Unlike the ordinary 2HDM, the leading result in the SI-2HDM does not same as the leading one in the SM even in the case that $\beta - \alpha = \pi/2$, which reflects the different origins of the electroweak symmetry breaking.

IV. SPHALERON DECOUPLING CONDITION AND CRITICAL BUBBLES

In EWBG, in order to preserve the generated BAU until today, the sphaleron process must be decoupled right after the electroweak symmetry breaking. This condition (the so-called sphaleron decoupling condition) is given by

$$\Gamma_B^{(b)}(T) < H(T), \quad (18)$$

where $\Gamma_B^{(b)}(T)$ is the baryon number changing rate in the broken phase, and $H(T)$ is the Hubble constant. Eq. (18) can be translated into

$$\frac{v(T)}{T} > \frac{g_2}{4\pi\mathcal{E}(T)} \left[42.97 + \log \mathcal{N} - 2 \log \left(\frac{T}{100 \text{ GeV}} \right) + \dots \right] \equiv \zeta_{\text{sph}}(T), \quad (19)$$

where the sphaleron energy is denoted as $E_{\text{sph}} = 4\pi v(T)\mathcal{E}(T)/g_2$, with g_2 being the SU(2) gauge coupling. \mathcal{N} represents the translational and rotational zero-mode factors of the fluctuations about the sphaleron.

In our numerical analysis, we first evaluate both T_C and v_C , where T_C stands for a critical temperature at which the two degenerate minima appear in the effective potential, and v_C is the VEV of the Higgs fields at T_C . The EWPT is studied in the direction of φ , and $\tan\beta$ is fixed by that at $T = 0$. We use the resummed finite-temperature one-loop effective potential

$$V_{\text{eff}}(\varphi, T) = \sum_i n_i \left[\frac{\bar{M}_i^4(\varphi, T)}{64\pi^2} \left(\log \frac{\bar{M}_i^2(\varphi, T)}{\bar{\mu}^2} - c_i \right) + \frac{T^4}{2\pi^2} I_{B,F} \left(\frac{\bar{M}_i^2(\varphi, T)}{T^2} \right) \right], \quad (20)$$

where

$$I_{B,F}(a^2) = \int_0^\infty dx x^2 \log \left(1 \mp e^{-\sqrt{x^2+a^2}} \right), \quad (21)$$

with the upper (lower) sign for bosons (fermions). $\bar{M}_i^2(\varphi, T)$ are the thermally corrected boson masses defined as $\bar{M}_i^2(\varphi, T) = \bar{m}_i^2(\varphi) + \Pi_i(T)$ where $\Pi_i(T)$ are the finite-temperature self-energy. Here, we consider the leading $\mathcal{O}(T^2)$ terms [27]

$$\Pi_\Phi(T) = \frac{T^2}{12v^2} \left[6m_W^2 + 3m_Z^2 + m_H^2 + m_A^2 + 2m_{H^\pm}^2 + 6(m_t^2 + m_b^2) \right], \quad (22)$$

$$\Pi_W(T) = 2g_2^2 T^2, \quad \Pi_B(T) = 2g_1^2 T^2, \quad (23)$$

where Π_Φ for the Higgs bosons, Π_W and Π_B for the SU(2) and U(1) gauge bosons, respectively. Note that the only longitudinal part of the gauge boson self-energy is thermally corrected.

After finding T_C , we evaluate the sphaleron energy at that temperature (for a detailed calculation, see, e.g.,

Refs. [28–30]). Since the dominant contribution in the right-handed side of Eq. (19) comes from $\mathcal{E}(T)$, we neglect the logarithmic terms in our numerical analysis.

It should be noted that the EWPT does not start at $T = T_C$. In order for the EWPT to occur, the bubbles must be nucleated at somewhat below T_C . Only bubble that has some critical size, which is called the critical bubble, can grow. The EWPT proceeds to develop if the bubble nucleation rate is larger than a certain value, and then the Universe is finally filled with the broken phase. We define the nucleation temperature (T_N) by the condition

$$\Gamma_N(T_N)/H^3(T_N) = H(T_N), \quad (24)$$

where $\Gamma_N(T_N)$ denotes the bubble nucleation rate per unit time per unit volume at T_N [31]. From Eq. (24), it follows that

$$\begin{aligned} & \frac{E_{\text{cb}}(T_N)}{T_N} - \frac{3}{2} \log \frac{E_{\text{cb}}(T_N)}{T_N} \\ &= 152.59 - 2 \log g_*(T_N) - 4 \log \left(\frac{T_N}{100 \text{ GeV}} \right), \end{aligned} \quad (25)$$

where $E_{\text{cb}}(T_N)$ is the energy of the critical bubble and $g_*(T_N)$ represents the degrees of freedom of the relativistic particles at T_N . As seen from Eq. (25), $E_{\text{cb}}/T \lesssim 150$ is needed for development of the EWPT.

We closely follow a method in [30] to evaluate $E_{\text{cb}}(T)$. The critical bubbles are estimated from the following energy functional

$$\begin{aligned} E_{\text{cb}}(T) = \int d^3 \mathbf{x} & \left[(\partial_i \Phi_1)^\dagger \partial_i \Phi_1 + (\partial_i \Phi_2)^\dagger \partial_i \Phi_2 \right. \\ & \left. + V_{\text{eff}}(\Phi_1, \Phi_2, T) \right], \end{aligned} \quad (26)$$

where the gauge fields are assumed to take the pure-gauge configuration so that they do not contribute to the energy of the critical bubbles. The classical Higgs fields are parametrized as

$$\Phi_1(r) = \frac{1}{\sqrt{2}} \begin{pmatrix} 0 \\ \rho_1(r) \end{pmatrix}, \quad \Phi_2(r) = \frac{1}{\sqrt{2}} \begin{pmatrix} 0 \\ \rho_2(r) \end{pmatrix}, \quad (27)$$

where $\rho_1(r) = \rho(r) \cos \beta$, $\rho_2(r) = \rho(r) \sin \beta$, $r = |\mathbf{x}|$, and here $\tan \beta$ is fixed by that at $T = 0$ as mentioned above. In the numerical analysis, it is convenient to change r and ρ_i into the following dimensionless quantities:

$$\xi = v(T)r, \quad h_1(\xi) = \frac{\rho_1(r)}{v(T) \cos \beta}, \quad h_2(\xi) = \frac{\rho_2(r)}{v(T) \sin \beta}. \quad (28)$$

The profiles of $h_i(\xi)$ are obtained by solving the equations of motion

$$-\frac{1}{\xi^2} \frac{d}{d\xi} \left(\xi^2 \frac{dh_{1(2)}}{d\xi} \right) + \frac{1}{v^4(T) \cos^2 \beta (\sin^2 \beta)} \frac{dV_{\text{eff}}}{dh_{1(2)}} = 0, \quad (29)$$

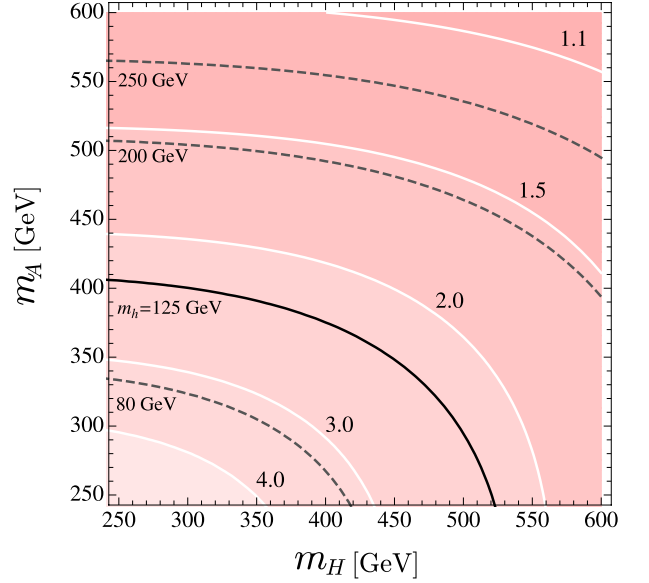


FIG. 1. Contours of the Higgs boson mass and v_C/T_C in the (m_H, m_A) plane. The solid line in black corresponds to $m_h = 125$ GeV, and the dashed lines in gray indicate $m_h = 80, 200$ and 250 GeV from bottom to top. The each contour in white represents $v_C/T_C = 1.1, 1.5, 2.0, 3.0$ and 4.0 from top to bottom.

with the boundary conditions: $dh_{1,2}(\xi)/d\xi|_{\xi=0} = 0$ and $h_{1,2}(\xi = \infty) = 0$. With those solutions, $E_{\text{cb}}(T)$ is evaluated.

It is known that the bubble solutions are approximately given by a kink-configuration

$$\rho_i(r) \sim v_i(T) \left[1 - \tanh \left(\frac{r-R}{L_w} \right) \right], \quad (30)$$

where R and L_w are the radius and wall width of the bubbles, respectively. We use this as the initial configuration to derive the bubble solutions by using the relaxation method. For more details about the numerical method, see, e.g., Ref. [30].

V. NUMERICAL RESULTS

In the SI-2HDM, there are five parameters in the tree-level potential:

$$\lambda_1, \quad \lambda_2, \quad \lambda_3, \quad \lambda_4, \quad \lambda_5. \quad (31)$$

In our analysis, we replace them with the following physical parameters:

$$m_H, \quad m_A, \quad m_{H^\pm}, \quad \beta, \quad v. \quad (32)$$

We take $m_{H^\pm} = m_A$ as mentioned in section II. Since V_{eff} does not depend on $\tan \beta$ explicitly, the results obtaining from it do not either, except for the cutoff of the model, as will be discussed in the following.

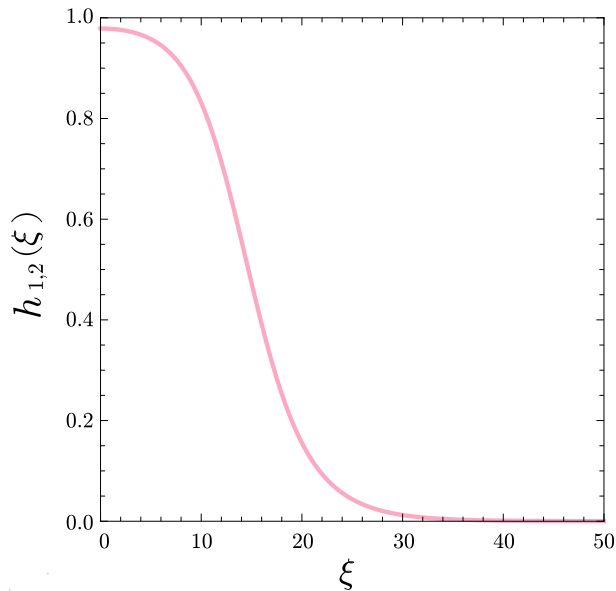


FIG. 2. Bubble profiles of $h_{1,2}(\xi)$ at $T = T_N$. In this plot, we set $m_h = 125$ GeV and $m_H = m_A = 382$ GeV.

In Fig. 1, we show the contours of the Higgs boson mass and v_C/T_C in the (m_H, m_A) plane. The black solid (gray dashed) line indicates the parameter region where $m_h = 125$ (80, 200, 250) GeV. As can be seen from Eq. (12), the Higgs boson mass gets larger as m_H and m_A increase. The white contours represent the magnitude of v_C/T_C . These contours indicate that the size of v_C/T_C becomes smaller as m_H and m_A get heavier. Since the thermal effects from the heavy Higgs bosons cause the first-order EWPT in this model, v_C/T_C would be proportional to $v \sum_i m_i^3 / \sum_i m_i^4$, $i = H, A, H^\pm$, from the high-temperature approximation argument. This may explain the behavior of v_C/T_C qualitatively. As a benchmark point, we take $m_h = 125$ GeV and $m_H = m_A = 382$ GeV. In this case, we find that $v_C/T_C = 211$ GeV/91.5 GeV = 2.31 and $\zeta_{\text{sph}}(T_C) = 1.23$. Therefore, even though ζ_{sph} is greater than the conventional criterion by 23%, v_C/T_C is large enough to satisfy the sphaleron decoupling condition. It is also found that $\zeta_{\text{sph}}(T_C)$ is almost constant on the black line while v_C/T_C gets slightly weaker in the region where $m_H \gtrsim 500$ GeV since the thermal effect of H loop is suppressed.

In Fig. 2, the profiles of $h_{1,2}(\xi)$ is shown, here $h_1(\xi) = h_2(\xi)$ by construction. Our numerical calculation shows that $v_N/T_N = 229$ GeV/77.8 GeV = 2.94, $\zeta_{\text{sph}}(T_N) = 1.20$ and $E_{\text{cb}}(T_N)/T_N = 151.7$. The degrees of the supercooling is about 15%, i.e., $(T_C - T_N)/T_C = 0.15$, which is more or less the same as the previous estimate [12].

Let us briefly make a comparison between the SI-2HDM and the minimal supersymmetric SM (MSSM). Unlike the SI-2HDM, the supercooling in the MSSM case is rather small, e.g., $\mathcal{O}(10^{-3})$ [30], and the bubble wall width in the SI-2HDM is thinner than that in the MSSM, which is due to the stronger first-order EWPT compared

m_H	382 GeV
v_C/T_C	211 GeV/91.5 GeV = 2.31
$\zeta_{\text{sph}}(T_C)$	1.23
v_N/T_N	229 GeV/77.8 GeV = 2.94
$\zeta_{\text{sph}}(T_N)$	1.20
$E_{\text{cb}}(T_N)/T_N$	151.7
κ_V	1.0
κ_f	1.0
$\mu_{\gamma\gamma}$	0.90
$\Delta\lambda_{hhh}$	82.1%
Λ	6.3 TeV

TABLE I. The benchmark point for the strong first-order EWPT and the nucleation of the bubbles, where we take $m_h = 125$ GeV and $m_H = m_A = m_{H^\pm}$. For the evaluation of Λ , $\tan \beta = 1$ is used.

to the MSSM case. Since a CP violating source term may be proportional to the gradient of the bubble wall [2], the baryon number generation may be more efficient than the MSSM case. To this end, of course, the current model has to be extended to have an extra source of CP violation.

In Table I, our numerical results in a benchmark point are summarized. In the SI-2HDM, the strong first-order EWPT is the inevitable consequence from the requirement of the 125 GeV Higgs boson. In this case, the significant deviations may appear in $\mu_{\gamma\gamma}$ and λ_{hhh} . We leave the study on the detectability of the heavy Higgs bosons to future work.

Finally, we comment on the cutoff scale (Λ) of this model. Here, Λ is determined by a scale at which $|\lambda_i| > 4\pi$ is obtained. In doing so, we use the one-loop renormalization group equations [32]. As an example, $\tan \beta = 1$ is taken. It is found that $\Lambda = 6.3$ TeV, which is extremely low compared to a typical grand unification scale, $\sim 10^{16}$ GeV. Since $\lambda_1 \propto \tan^2 \beta$ and $\lambda_2 \propto 1/\tan^2 \beta$, the cases for $\tan \beta > 1$ and $\tan \beta < 1$ yield the lower cutoff scales than 6.3 TeV. Our analysis has reconfirmed the previous results [14, 16].

VI. CONCLUSIONS AND DISCUSSIONS

We have revisited the EWPT and the profiles of the critical bubbles in the SI-2HDM in the light of the 125 GeV Higgs boson. We improved these analyses by using the finite temperature one-loop effective potential with thermal resummation. In this model, the heavy Higgs mass scales are fixed to be consistent with the $m_h = 125$ GeV. In our benchmark point, $m_H = m_A = m_{H^\pm} = 382$ GeV, we found that $v_C/T_C = 211$ GeV/91.5 GeV = 2.31 and $\zeta_{\text{sph}}(T_C) = 1.23$. At the nucleation temperature, they are changed into $v_N/T_N = 229$ GeV/77.8 GeV = 2.94 and $\zeta_{\text{sph}}(T_N) = 1.20$. Even though ζ_{sph} in the SI-2HDM is greater than the conventional criterion by about 20%, the first-order EWPT is strong enough to satisfy the sphaleron decoupling condition.

We also studied the deviations of the Higgs boson cou-

plings from the SM predictions. It was found that even though the Higgs boson couplings to the gauge bosons and fermions are SM like, the significant deviations may appear in the $h \rightarrow \gamma\gamma$ mode and the triple Higgs boson coupling due to the nondecoupling effects of the heavy Higgs boson loops. In our benchmark point, the Higgs signal strength of $h \rightarrow \gamma\gamma$ is reduced by 10% and the triple Higgs boson coupling is enhanced by 82.1%. Such deviations may be detectable in the future experiments such as the High-Luminosity LHC [7] and the ILC [8].

There are some issues to be solved. In order to obtain the baryon asymmetry, an extra source of CP violation is needed as mentioned in the previous section. To this end, we may augment this model by adding the extra fermions in a scale-invariant way. The current analysis would not be much modified as long as the strength of the

interactions between new particles and the Higgs boson are moderate. Furthermore, since the cutoff of the model is rather small, the UV completion is needed. However, constructing a complete model is beyond the scope of this Letter.

ACKNOWLEDGMENTS

The work of K.F. is supported by Research Fellowships of the Japan Society for the Promotion of Science for Young Scientists. E.S. is supported in part by the Ministry of Science and Technology of R. O. C. under Grant No. MOST 104-2811-M-008-011.

-
- [1] P. A. R. Ade *et al.* [Planck Collaboration], *Astron. Astrophys.* **571**, A16 (2014).
 - [2] V. A. Kuzmin, V. A. Rubakov and M. E. Shaposhnikov, *Phys. Lett. B* **155** (1985) 36. For reviews on electroweak baryogenesis, see A. G. Cohen, D. B. Kaplan and A. E. Nelson, *Ann. Rev. Nucl. Part. Sci.* **43** (1993) 27; M. Quiros, *Helv. Phys. Acta* **67** (1994) 451; V. A. Rubakov and M. E. Shaposhnikov, *Usp. Fiz. Nauk* **166** (1996) 493; K. Funakubo, *Prog. Theor. Phys.* **96** (1996) 475; M. Trodden, *Rev. Mod. Phys.* **71** (1999) 1463; W. Bernreuther, *Lect. Notes Phys.* **591** (2002) 237; J. M. Cline, [arXiv:hep-ph/0609145]; D. E. Morrissey and M. J. Ramsey-Musolf, *New J. Phys.* **14**, 125003 (2012); T. Konstandin, *Phys. Usp.* **56** (2013) 747 [*Usp. Fiz. Nauk* **183** (2013) 785].
 - [3] G. Aad *et al.* [ATLAS Collaboration], *Phys. Lett. B* **716**, 1 (2012).
 - [4] S. Chatrchyan *et al.* [CMS Collaboration], *Phys. Lett. B* **716**, 30 (2012).
 - [5] G. Aad *et al.* [ATLAS and CMS Collaborations], arXiv:1503.07589 [hep-ex].
 - [6] T. Cohen, D. E. Morrissey and A. Pierce, *Phys. Rev. D* **86**, 013009 (2012); D. Curtin, P. Jaiswal and P. Meade, *JHEP* **1208**, 005 (2012); M. Carena, G. Nardini, M. Quiros and C. E. M. Wagner, *JHEP* **1302**, 001 (2013); K. Krizka, A. Kumar and D. E. Morrissey, arXiv:1212.4856 [hep-ph].
 - [7] [CMS Collaboration], arXiv:1307.7135; [ATLAS Collaboration], arXiv:1307.7292 [hep-ex].
 - [8] H. Baer, T. Barklow, K. Fujii, Y. Gao, A. Hoang, S. Kanemura, J. List and H. E. Logan *et al.*, arXiv:1306.6352 [hep-ph].
 - [9] S. R. Coleman and E. J. Weinberg, *Phys. Rev. D* **7** (1973) 1888.
 - [10] E. Gildener and S. Weinberg, *Phys. Rev. D* **13** (1976) 3333.
 - [11] K. Inoue, A. Kakuto and Y. Nakano, *Prog. Theor. Phys.* **63** (1980) 234.
 - [12] K. Funakubo, A. Kakuto and K. Takenaga, *Prog. Theor. Phys.* **91**, 341 (1994).
 - [13] K. Takenaga, *Prog. Theor. Phys.* **92** (1994) 987.
 - [14] K. Takenaga, *Prog. Theor. Phys.* **95** (1996) 609.
 - [15] J. S. Lee and A. Pilaftsis, *Phys. Rev. D* **86** (2012) 035004.
 - [16] C. T. Hill, *Phys. Rev. D* **89** (2014) 7, 073003.
 - [17] S. Kanemura, Y. Okada and E. Senaha, *Phys. Lett. B* **606** (2005) 361.
 - [18] K. Fuyuto and E. Senaha, *Phys. Rev. D* **90**, no. 1, 015015 (2014).
 - [19] S. L. Glashow and S. Weinberg, *Phys. Rev. D* **15** (1977) 1958.
 - [20] R. Jackiw, *Phys. Rev. D* **9**, 1686 (1974).
 - [21] H. E. Haber and A. Pomarol, *Phys. Lett. B* **302**, 435 (1993); A. Pomarol and R. Vega, *Nucl. Phys. B* **413**, 3 (1994); P. H. Chankowski, M. Krawczyk and J. Zochowski, *Eur. Phys. J. C* **11**, 661 (1999); J.-M. Gerard and M. Herquet, *Phys. Rev. Lett.* **98**, 251802 (2007); W. Grimus, L. Lavoura, O. M. Ogreid and P. Osland, *Nucl. Phys. B* **801**, 81 (2008); S. de Visscher, J. M. Gerard, M. Herquet, V. Lemaître and F. Maltoni, *JHEP* **0908**, 042 (2009).
 - [22] I. F. Ginzburg, M. Krawczyk and P. Osland, In *Seogwipo 2002, Linear colliders* 90-94 [hep-ph/0211371].
 - [23] D. McKeen, M. Pospelov and A. Ritz, *Phys. Rev. D* **86** (2012) 113004.
 - [24] J. F. Gunion, H. E. Haber, G. L. Kane and S. Dawson, *Front. Phys.* **80** (2000) 1.
 - [25] S. Kanemura, S. Kiyoura, Y. Okada, E. Senaha and C. P. Yuan, *Phys. Lett. B* **558** (2003) 157; S. Kanemura, Y. Okada, E. Senaha and C.-P. Yuan, *Phys. Rev. D* **70** (2004) 115002.
 - [26] D. Chway, T. H. Jung, H. D. Kim and R. Dermisek, *Phys. Rev. Lett.* **113** (2014) 5, 051801.
 - [27] M. E. Carrington, *Phys. Rev. D* **45**, 2933 (1992).
 - [28] N. S. Manton, *Phys. Rev. D* **28**, 2019 (1983).
 - [29] F. R. Klinkhamer and N. S. Manton, *Phys. Rev. D* **30**, 2212 (1984).
 - [30] K. Funakubo and E. Senaha, *Phys. Rev. D* **79** (2009) 115024.
 - [31] A. D. Linde, *Nucl. Phys. B* **216**, 421 (1983) [Erratum-ibid. B **223**, 544 (1983)].
 - [32] G. C. Branco, P. M. Ferreira, L. Lavoura, M. N. Rebelo, M. Sher and J. P. Silva, *Phys. Rept.* **516** (2012) 1.